JOURNAL OF MATERIALS SCIENCE 31 (1996) 6595–6607

Laser welding of Al55–Zn coated steel sheet

J. M. AMO, J. DURÁN, J. CHAO, J. FERNÁNDEZ-SÁEZ
Centro Nacional de Investigaciones Metalúrgicas (CENIM) – CSIC Avda, Gregorio del Amo, 8. 28040 Madrid, Spain

A study has been made of the procedures used for the lap and butt welding of 0.62 and 1.16 mm thickness steel sheets coated with Al55–Zn alloy, using laser-beam technology. The main problems arise in lap welding as a result of zinc evaporation from the coating. The vapour pressures of this element lead to cratering and blistering of the welds which are visible from the external surface and imply severe weld defects. An efficient solution to this problem consists in leaving a gap between the internal faces, thus allowing the zinc vapours to escape. Excessive gaps, however, lead to the molten metal collapse and to lack of penetration. In the present work, acceptable results were obtained with a maximum interface separation of 0.1 mm. This allows excellent continuity of the joints, without cracks, pores or non-metallic inclusions and with moderate hardnesses, thus demonstrating the good laser weldability of the coated material. A difficulty arises, however, in relation to the coating in zones close to the weld. In these high-temperature zones the coating is lost, and in the immediately adjacent areas the coating microstructure and phases are altered, as was shown by scanning electron microscope analyses.

1. Introduction

The laser welding of coated sheets brings together two important aspects of new technologies currently under development. On the one hand there is the application of laser systems with sufficient power and control to melt and weld metals, and on the other the growing use of steel sheets with anti-corrosion protection. Of the latter, and in addition to the immersion-galvanized and electrogalvanized materials based on zinc, Zn–Fe, Zn–Fe–Ni, etc., there is growing interest in Al–Zn coating containing different quantities of aluminium, because of its greater resistance to corrosion [1, 2].

Incorporation of these new anti-corrosion materials in the classical automotive, household appliance, rail and naval industries, among others, has provided unquestionable improvements in the durability and quality of the resulting products, but has also meant certain difficulties in the classical manufacturing processes used, especially in relation to resistance spot welding. The main problem caused in this respect is related to the rapid deterioration of the electrode tips, this giving rise to an important lack of regularity in the dimensions and quality of the spots welded.

In the case of laser welding of coated sheet there is a different problem in relation to welding of the bare sheet. The coating constitutes an interference especially in relation to lap welding, which is the technique most directly comparable to spot welding, but has hardly any impact on the quality of butt welds.

In the case of resistance welding, the problem may be palliated by different means. For example, periodic machining of the electrode tips, the use of weld current pulses with up-slope and down-slope controls and the application of pre-programmed step increases in welding intensity. Other measures affect the shape or material of the electrodes, particularly for welding of Al–Zn range coating. The aluminium present in such coating, normally in percentages ranging from 5%–55%, complicates the welding process because of the alumina, which contaminates the electrodes, especially in the case of high aluminium-content coatings. In these cases, the best results are obtained using pimple electrodes, sometimes made of materials having higher resistance to heat and to pitting, such as copper alloy with alumina dispersion or tungsten inserts [3–5].

Nevertheless, the troubles involved in this process persist. The laser, for its part, is seen to be an interesting alternative for the welding of this type of material, albeit subject to problems of its own. The characteristic advantages of this type of welding for thin sheet are unquestionable, due to its low heat input and high welding speed, which give rise to welds having a high depth/width ratio, with minimum heat-affected zones and very low residual stresses and deformations. Under suitable welding conditions and with adequate edge preparation, healthy welds with acceptable levels of ductility may be obtained, these even allowing for severe forming operations. In coated sheet, the damage to the coating is minimal because of the narrowness of the welds (usually $\leqslant 1$ mm).

The most important problems arise when sheets with defective joint adjustment or excessive separations are to be welded. In normal practice, the weld edges are prepared by shearing. In the case of butt welds, this may give rise to misalignments or to V-shaped bevels due to the shape of the sheared edges,

0022–2461

which in turn may cause different types of defects in the welds [6]. Similarly, in the case of lap joints, the bad fit-up at the interface gives rise to poor-quality welds, due to the lack of filling material or of penetration in the lower sheet. Some clearance between the sheets would appear to be necessary when welding coated steels, because an exit must be provided for the metallic vapours from the coating [7, 8].

This latter problem is, in fact, one of the basic difficulties currently involved in the laser welding of coated steels [9, 10]. In every case, depending on the nature and thickness of the coating, the thickness of the sheets and the welding conditions, there will be a compromise separation between the lap sheets allowing welds of the best characteristics to be obtained.

The lack of information on these aspects of the laser welding of protected sheets in general, and of aluminium-containing coating in particular (because of its less well-known weldability) has led us to undertake the present work. A study has been made of procedures for laser butt and lap welding of steel sheet having a protective coating of Al55–Zn, taking into consideration the mechanical and metallurgical characteristics of the welded joints and the damage induced in the coating.

2. Experimental procedure

The material used was sheet of extra-mild steel, 0.62 and 1.16 mm thick, for deep-drawing, coated on either face with a layer of Al55–Zn alloy measuring 35 μm rated thickness and manufactured by the Spanish Ensidesa steel works under the name Algafort. The chemical composition of the substrate and protecting layer is shown in Table I, the mechanical properties of the coating material being shown in Table II.

The welds were performed on samples measuring 150 mm in length and 40–80 mm in width, with the edges sheared. The lap welds were carried out on samples 0.62 mm thick and the butt welds on the samples of both thicknesses. The samples, previously cleaned with a solvent to eliminate contamination by greases, dust, etc., were then suitably held in a weld positioner with a central channel (Fig. 1) in order to allow the back of the welds to be shielded with inert gas. Shielding was afforded on the front by means of the plasma control gas, via a nozzle oriented concentrically to the laser beam. In both cases helium was used as a shielding gas because of its excellent capacity for plasma suppression, a property which facilitates both focusing of the beam and penetration of the welds. These were performed by moving the positioner beneath the laser head at the welding speed.

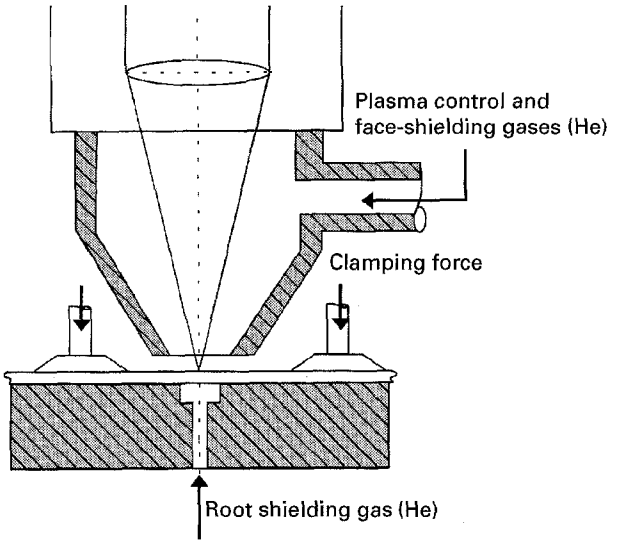

Figure 1 Welding positioner and gas shielding system.

The welding equipment was a Rofin-Sinar, 6 kW continuous CO_2 laser fitted with a parabolic mirror of 127 mm focal length. The tests were initiated in the TEM20 transmission mode, more suitable for thin-sheet welding, but in view of the poor results obtained and in order to achieve better focusing and reduce damage to the coating, continued in the TEM00 mode, the latter being used for practically all the tests performed. In this mode, the beam was focused on the surfaces of the parts, giving a molten focal area (operating spot) of approximately 0.22 mm. In view of the focal depth provided by this beam, $d \approx 2$ mm [10], which was greater than the maximum total thickness to be welded ($2 \times 0.62 = 1.24$ mm, in lap welding), it was not necessary to change the focusing depth for any of the tests.

Following welding, the joints were visually inspected to check the surface finish and for underfilling, undercuts, etc., and subjected to radiographic tests and die-penetrant inspection to determine the possible presence of cracking, porosity, incomplete fusion or inadequate joint penetration. These defects, along with the microstructures present and damage to the coating, were also studied using standard optical and electronic metallographic procedures. The values of hardness were determined using a microhardness meter allowing loads of 25 g to 10 kg to be applied, and the mechanical properties were determined by means of an MTS servohydraulic unit with a load cell of 250 kN. Finally, the maps showing the distribution of the elements in the different phases of the coating were drawn up by wavelength dispersion using a Jeol model JXA-840 scanning electron microscope.

TABLE I Chemical composition of the material (wt %)

	C	Mn	Si	P	S	Al	Zn
Substrate	0.017	0.28	< 0.05	0.004	0.009	< 0.001	–
Coating[a]			1.5			55	43.5

[a] Nominal values.

TABLE II Mechanical properties

Thickness (mm)	Yield strength (MPa)	Tensile strength (MPa)	Elongation (%)
0.62	320	370	43
1.16	350	400	39

3. Results and discussion

3.1. Welding procedures

3.1.1. Lap welds

The lap welds were performed on sheets 0.62 mm thick and 150 mm × 80 mm (length × width), with an overlapping zone of 45–55 mm wide along the shorter dimension. The sheets were held firmly in the welding positioner and a 14 l min^{-1} flow of helium was supplied for plasma control and the upper face shielding, along with a smaller 4 l min^{-1} flow via the positioner channel for back shielding.

The graph shown in Fig. 2 summarizes the results obtained under the different welding conditions used for optimization of the lapping procedure, depending on the power of the laser beam and the welding speed.

In the TEM20 transmission mode, focusing on sheet surface (dotted area in the graph) with a minimum operating spot of some 0.40 mm, it was not possible to achieve adequate lower sheet penetration, in spite of the relatively high beam powers used (more than 2 kW). The heat generated caused the coating to evaporate on either side of the weld on a width equivalent to the thickness of the sheet. Fig. 3 shows these weld characteristics.

The experiments were continued in the TEM00 mode with a view to achieving better penetrations and smaller coating losses, due to the improved beam focusing that may be achieved in this transmission mode. The beam was concentrated on the surface of the sheets, with a focal spot of approximately 0.22 mm being obtained.

Returning to the previous graph, it may be seen that with powers equal to or greater than 2 kW and welding speeds of 4–5.5 m min^{-1}, heat input is still excessive, with perforation of the sheets and spattering of the molten material. Fig. 4 shows a sample of these results. By increasing the speed it is possible to maintain the melted weld pool, but the beam produces strong undercuts at the surface.

Suitable welding conditions are achieved with powers of between 1.2 and 1.7 kW. Depending on the power level used, total or partial penetration welds are obtained. Fig. 5 shows the cross-sections of two welds obtained within this power range. At powers of less than 1.2 kW, penetration is irregular with fusion lacks at the lower sheet occurring, as shown in the graph. A minimum power of 1 kW is required for the beam to begin weld penetration. Otherwise, and even at low speeds (2 m min^{-1}) what is achieved is a widening of the melting zone at the upper surface and overheating of the materials.

In the area of acceptable welding conditions, however, there is a major difficulty which prevents correct formation of the welds. The problem is one of vaporization of the zinc in the Al–Zn coating on the inner surfaces of the sheets in the area of the joint. The

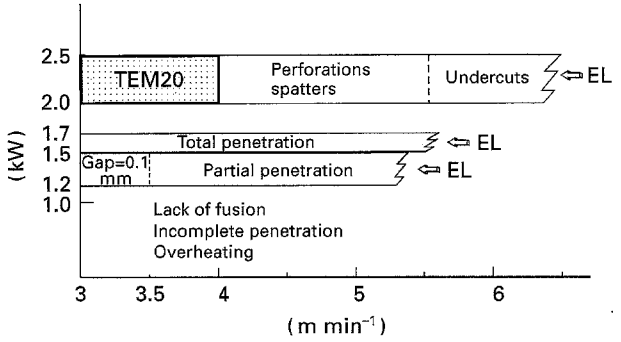

Figure 2 Lap-weld features according to the beam power and welding speed. Dotted area, TEM20 mode; remaining graph, TEM00 mode; EL, experiment limits.

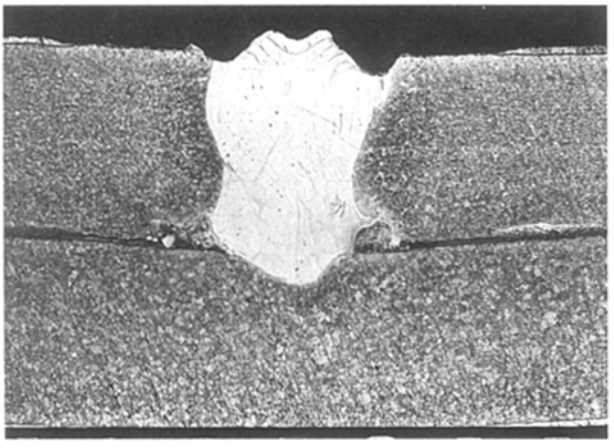

Figure 3 Cross-section of a weld made in TEM20 mode, × 50.

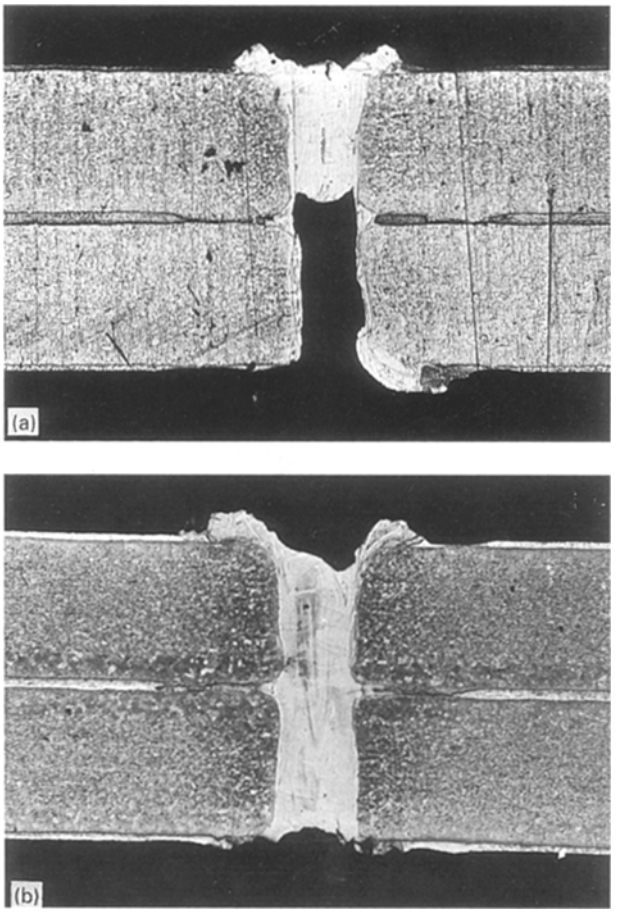

Figure 4 (a) Perforation of the lower sheet. (b) Underfilling due to blow-out of weld metal at the upper surface welding conditions 2 kW, 5 m min^{-1}.

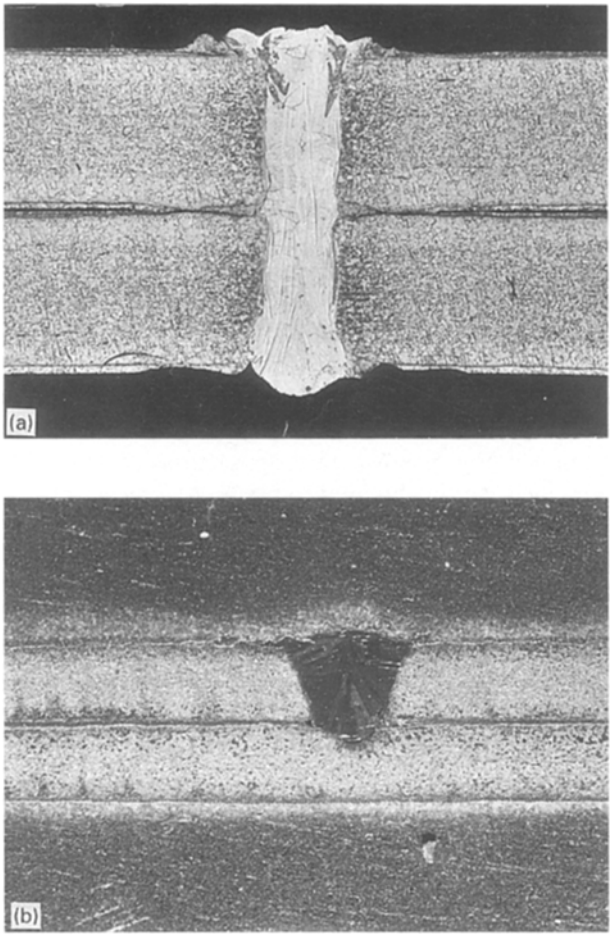

Figure 5 (a) Total penetration weld, 1.7 kW, 5 m min^{-1}. (b) Partial penetration weld, 1.4 kW, 4 m min^{-1}.

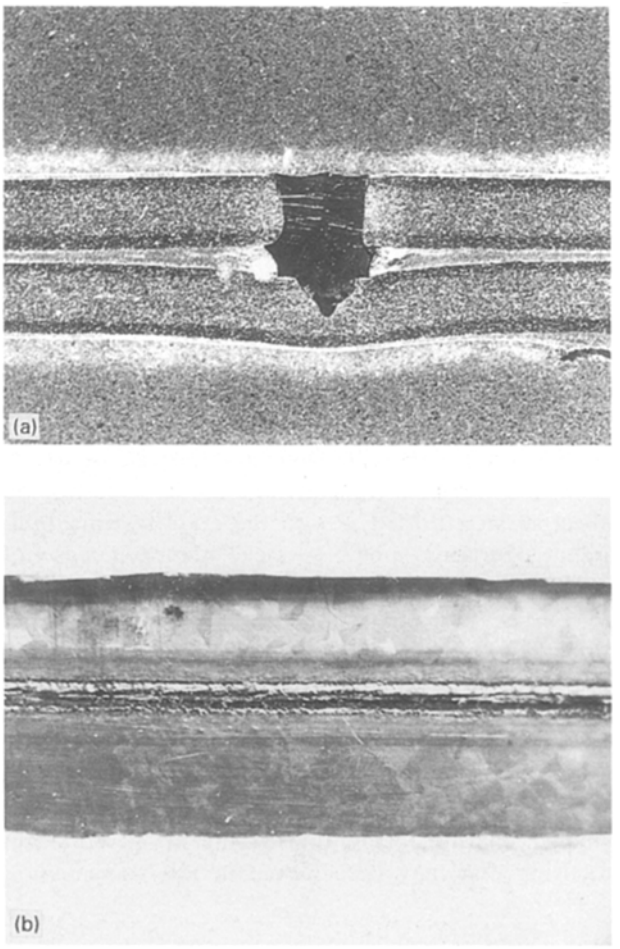

Figure 6 Lap weld made with 0.1 mm interface gap, 1.5 kW, 3.3 m min^{-1}. (a) Cross section, (b) surface appearance.

pressure of the vapours formed is capable of expelling the molten metal, giving rise to defects such as underfilling and lack of penetration, pores and bulging or blistering at the surface of the welds. In order to avoid this, it is necessary to leave an exit path for the vapours providing a small gap at the joint interface. In this work, this solution has been studied for partial penetration welds, this being developed further in a later section. Suffice it to say here that the best welds were achieved with a interface gap of 0.1 mm, at the same power levels as used previously for joints with close fit-up and at somewhat lower speeds, 3–3.5 m min^{-1}. Fig. 6a shows a sample of the penetration produced under these conditions, while Fig. 6b shows the surface appearance of these welds.

The essential difference between these welds is that in the case of joints with close fit-up (Fig. 5b) the penetration depth is not constant and is frequently interrupted by interface vaporization of the coating. Externally, the effect of this vaporization is the formation of blisters on the surface of the weld, as will be seen below in the study of weld defects.

Table III shows the conditions of the lap-welding procedures for total penetration, partial penetration without interface separation and partial penetration with an interface gap of 0.1 mm. The mechanical characteristics of the three types of welds were determined using tension–shear type test specimens with a transverse weld (Fig. 7a) the results being shown in Table IV. The calculation was performed using the thickness of a single sheet (0.62 mm) as the reference strength area, with a view to comparing the results with those obtained from the base material, which showed a minimum tension strength of 370 MPa. The best values were obtained with the gap of 0.1 mm–297 MPa. The lowest values for no-gap joints were due to the lack of regularity in the melting of these welds. In all cases, failure occurred throughout the heat-affected zone due to the fact that during testing the sheets tend to align in the direction of the load line, with deformation concentrating in the lower sheet, alongside the weld. Fig. 7b shows this typical rupture form in these test pieces.

TABLE III Parameters of the three lap-weld procedures. IG = interface gap, sheet thickness = 0.62 mm, plasma control and face shielding (He) = 14 l min^{-1}, root shielding (He) = 4 l min^{-1}, transmission mode TEM00

	Total penetration	Partial penetration	
		IG = 0	IG = 0.1
Power (kW)	1.5–1.7	1.2–1.5	1.2–1.5
Speed (m min^{-1})	3.8–5.5	3.5–5.5	3–3.5
Heat input (J mm^{-1})	25–18	20–26	24–26

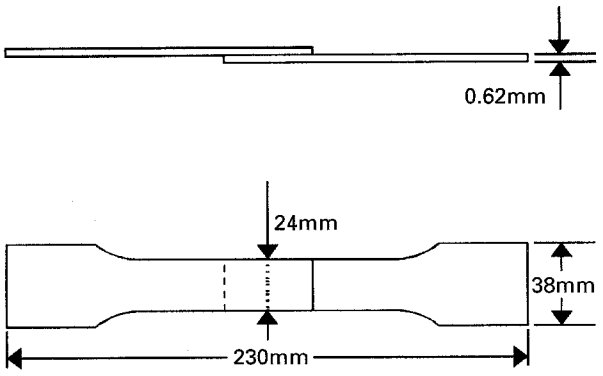

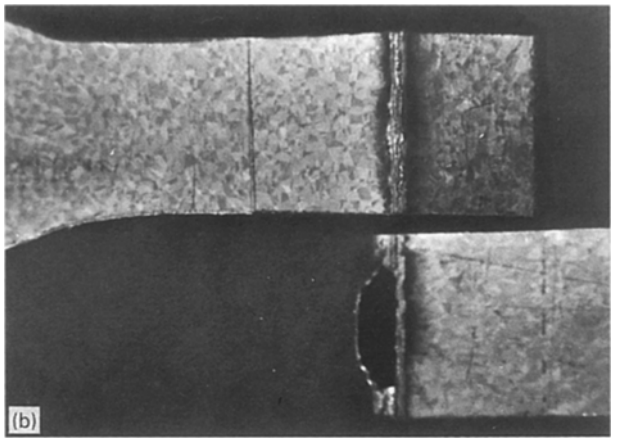

Figure 7 Tension–shear specimens for lap-welding testing. (a) Specimen layout, (b) typical failure.

TABLE IV Tensile strength of the three types of welds (average of three values). IG = interface gap. Base material strength = 370 MPa

Type of weld	Strength (MPa)
Total penetration	233
Parital penetration: IG = 0	241
IG = 0.1	297

3.1.2. Butt welds

The study of the power for this welding procedure was accomplished using weld beads by means of laser-beam penetration on sheets 0.62 mm thick. The minimum power required to achieve total penetration at the welding speed without sheet cutting or weld perforation, or even excessive root reinforcement of the molten metal, was determined. Using the TEM00 mode, with beam focusing on the surface and a focal spot of 0.22 mm, the power range for these conditions was established at between 700 and 800 W, at a welding speed of 4 m min^{-1}.

Final adjustment was made on the basis of actual autogenous butt-welding tests on sheets with no gap between joint faces. Sheets measuring 150 mm × 80 mm were used, duly positioned in the device shown in Fig. 1. The joint edges were not previously machined but were used directly with the finish provided by the sheet-shearing process. The optimum

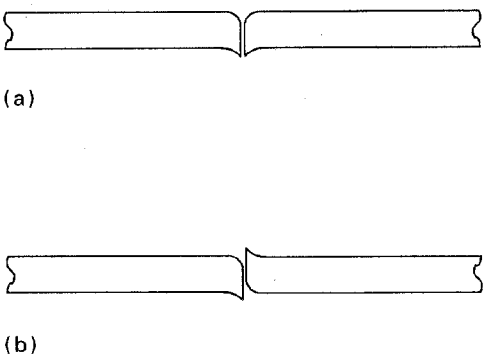

Figure 8 Weld shear cut edges arrangement: (a) direct position, (b) inverted position.

conditions were obtained with a power of 800 W and at a welding speed of 3.8 m min^{-1}.

An observation should be made with respect to the direct use of shear cuts. Given that the upper angles of the cutting edge are left rounded, this type of cut may give rise to weld defects. In keeping with suggestions made by certain researchers [4], the parts to be welded were coupled by inverting the cutting face of one of them, such that the sections of the joint faces were essentially parallel (Fig. 8b). This favoured the balance of the melted material at the face and root of the weld. The use of the position in Fig. 8a can cause underfilling and sagging of the welds. Another possibility normally giving good results is to use the direct shear edges position and weld with the face-down up, relative to Fig. 8a.

The welding procedure for the 1.16 mm thickness was studied using a similar systematic approach, the same behaviour being observed as regards the configuration of the shear edges. The better conditions from the point of view of weld penetration and surface finish were obtained with a power of 1300 W and a weld speed of 1.4 m min^{-1}.

The mechanical characteristics of both thicknesses, determined using transverse tension test specimens, were according to the strength of their respective base materials, with failure occurring away from the welds at values in excess of those corresponding to such base materials: 370 MPa and 400 MPa for the 0.62 mm and 1.16 mm thicknesses, respectively.

Fig. 9a and b show the surface appearance of the face and root, respectively, of one of the welds performed on the 0.62 mm thick sheet, while Fig. 9c shows the shape of the penetrations of these joints. Finally, Table V summarizes the optimum welding parameters for both thicknesses.

3.2. Weld defects

To the defects commonly found in laser-welded bare steels due to the inadequate adjustment of the weld parameters, edge preparation, etc., such as undercutting, lack of penetration, porosity, misalignment, etc., are to be added, in the case of coated steels, a series of specific defects arising as a result of the coating itself. A study has been made of the defects encountered in the welds carried out for the optimization of the

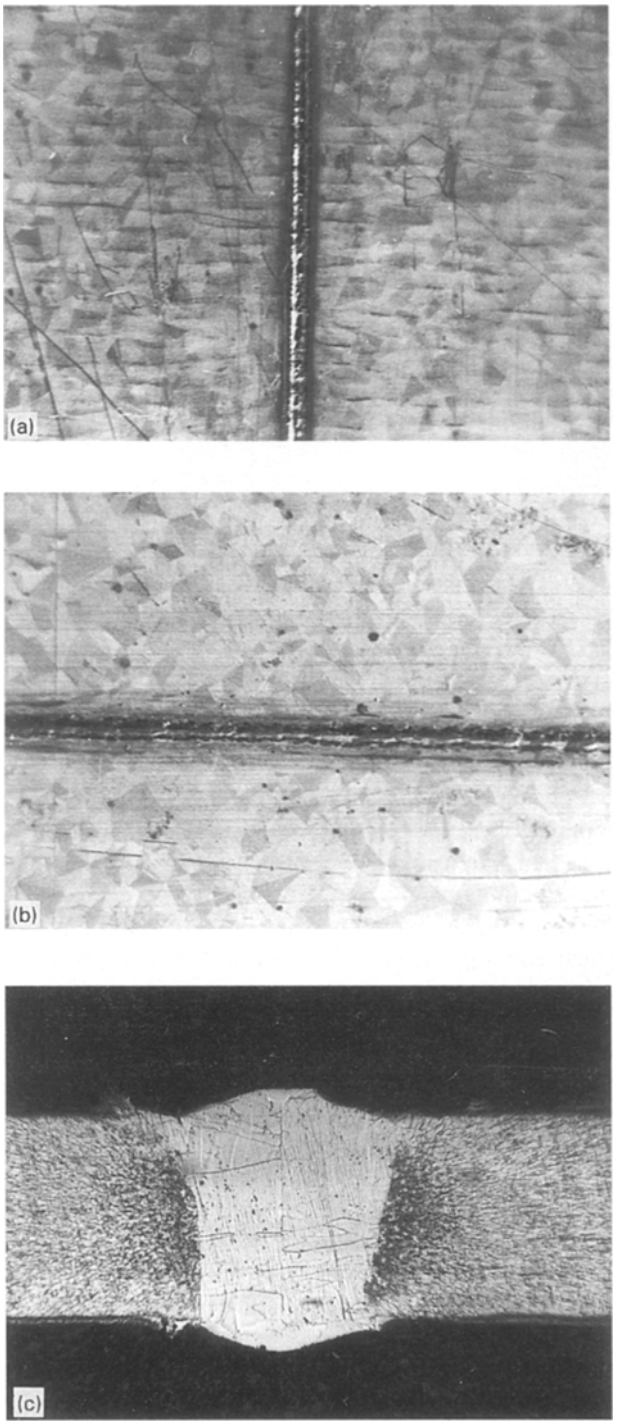

Figure 9 Butt welds in 0.62 mm thickness sheet. (a) Weld face, (b) weld root, (c) cross-section.

TABLE V Optimum parameters for butt welding procedures. Plasma control and face shielding (He) = 14 l min^{-1}. Root shielding (He) = 4 l min^{-1}. Transmission mode = TEM00

	Thickness	
	0.62 mm	1.16 mm
Power (kW)	0.8	1.3
Speed (m min^{-1})	3.8	1.4
Heat input (J mm^{-1})	12.6	55.7

previous procedures, with special analysis of the defects caused by Al55–Zn coating. In view of the different problems posed, lap and butt welds will be considered separately.

3.2.1. Lap welds

In the case of both butt and lap welds, the Al–Zn coating was observed to disappear from the areas of the sheet surfaces close to the welds. Given that zinc boils at 900 °C and that this does not occur with aluminium until 2450 °C, it may be assumed that in these areas the zinc volatilizes while the aluminium simply melts, at a temperature of 660 °C, except in the welds themselves, where boiling temperature may be reached. In these areas, therefore, the disappearance of the coating may be due to the volatilization of zinc, on the one hand, and to displacement of the liquid aluminium, on the other. On the outer surfaces, the displacement may be due to the flow of the shielding and plasma control gases, while on the inner surfaces it may be the result of the pressure of the zinc vapours, in the case of lap welding.

In this type of weld, the most frequent defects caused by the zinc vapours are craters and expulsions of molten metal, which at times are equivalent to actual cutting of the upper or lower joint sheets. Fig. 10 shows two examples of these defects: Fig. 10a shows the vapour outlet duct, which ends in a crater on the weld surface, while Fig. 10b shows the disappearance of the inner coating, which has expelled almost all the molten material from the upper sheet of the weld. Fig. 11a and b show two transverse sections of another weld, illustrating two successive positions of the molten material on its path to the outside in the case of a hypothetical explosion, as a result of the thrust provided by vapours from the coating. The absence of the latter at the inner surface of the sheets is also clear in Fig. 11b. In addition to the aforementioned defects, the pressure of the vapours may even cut the weld into two halves at the interface level, as may be noted in Fig. 12.

The existence of this type of defect is easy to detect visually, because bulging or blistering occurs at the weld surfaces. Figs 11a and b are, in fact, of the transverse sections of two of these blisters. The external appearance of these blisters may be seen in Fig. 13, which shows a weld area with three such defects. Each of these blisters is often accompanied by a crater, as may be seen in the same figure. The craters are normally located in front of the blisters in the weld direction, where the molten material is more fluid because of the proximity of the laser beam and where the vapours find the weakest area for exit.

As has been pointed out above, in order to provide an exit for the coating vapours and, therefore, prevent the occurrence of defects of this nature, it is advisable to perform welds with a slight clearance between sheets in galvanized steels. This was the solution adopted here, extended also to include Al55–Zn coating, through the incorporation of spacers between the sheets to be welded. Nevertheless, this simple solution required the study of a new welding procedure, in order to prevent the occurrence of other types of defects as serious as those commented on above. Given their interest in regard to understanding the effects that such spacers might produce, certain of the more significant tests which were performed allowing an optimum interface gap to be achieved for lap welding, are described below.

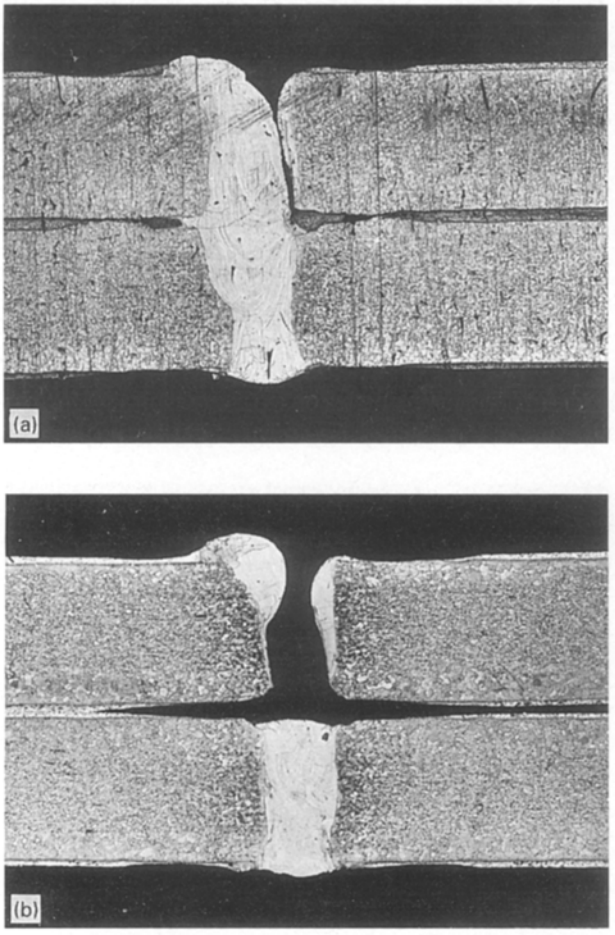

Figure 10 (a) Outlet duct of the coating vapours. (b) Expulsion of the weld-melted material.

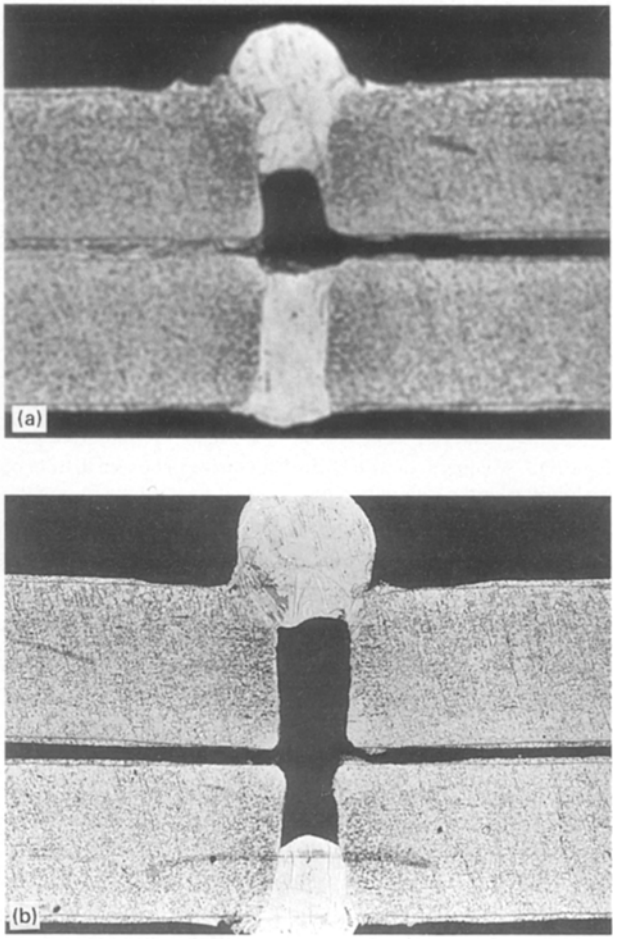

Figure 11 (a,b) Cross-sections of two blisters.

3.2.1.1. Effects of sheet clearance. In the initial close fit-up lap welds in 0.62 mm thickness, acceptable penetrations in the lower sheet were achieved with power levels of between 1.2 and 1.5 kW and speeds of 3.5–5.5 m min^{-1}, albeit with frequent expulsions of molten material and craterings and blistering of the weld surfaces. For the study of interface clearance, relatively high power conditions of 1.5 kW were selected, along with variable welding speeds of 4–2 m min^{-1} and gaps of 0.15 and 0.10 mm. The spacers used were inconel foils calibrated to these thicknesses and located 1 cm from the joint line.

With spacers of 0.15 mm it was not possible to achieve satisfactory welds, as is demonstrated by the macrosections shown in Fig. 14a–c, selected from tests performed at different speeds. The weld shown in Fig. 14a was performed at 3 m min^{-1} and melted an appreciable depth of the lower sheet but without a bond being formed between the molten material of both sheets, this producing a lack of continuity in the complete section of the weld at the inner faces. The weld shown in Fig. 14b, obtained at a speed of 2.5 m min^{-1}, shows acceptable penetration as a result of a greater heat input, but nevertheless presents also accentuated material underfill at the surface due to collapse of the molten material. When the speed was reduced to 2 m min^{-1}, weld material was expelled as a result of the excessive heat transferred. Fig. 14c includes a sample of the results of these expulsions from the weld.

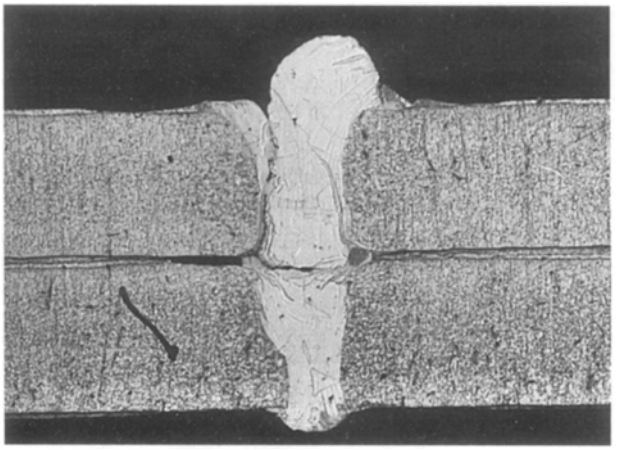

Figure 12 Loss of continuity of the weld material due to penetration of coating vapours at the interface level.

Without altering the power of the laser beam, 1.5 kW, the gap was changed to 0.1 mm. The welds obtained were of acceptable quality, in the case of weld speeds of between 3 and 3.5 m min^{-1}. Fig. 6 shows a representative example of the welds performed in this range of speeds. The sample corresponds to a weld carried out in 3.3 m min^{-1} and shows an intermediate penetration of those obtained in this range. The surface is smooth and uniform and free from blistering, unlike the welds performed with close fit-up between sheets, Fig. 13.

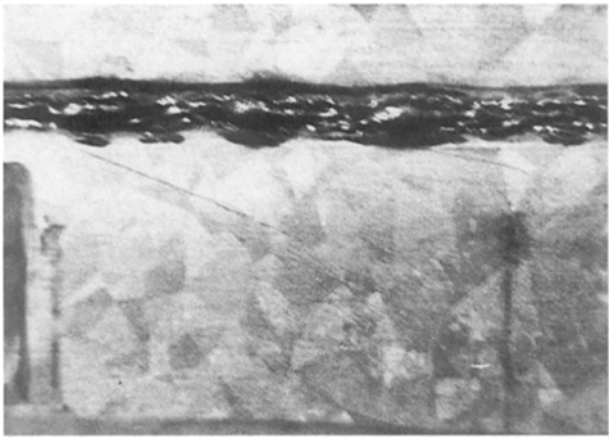

Figure 13 Welding area with blisters. A crater can be seen in front of each blister in the weld direction.

As a result of the aforementioned tests, it was deduced that the opening between the sheets due to the spacer was an efficient aid to the exit of the inner coating vapours, as demonstrated by the complete absence of blistering at the surface. If the separation is excessive, however, the layer of air created between the sheets makes it more difficult for heat transfer to occur to the lower sheet, this resulting in greater heat input requirements for acceptable degrees of penetration to be achieved. Frequently, these conditions cause molten material to be expelled, leaving unacceptable bubbles and cavities in the welds. When this does not occur, the surface of the weld collapses and underfill defects occur as a result of the limited molten material available to cover the separation. Correct choice of this parameter is, therefore, of the greatest importance. The 0.1 mm thickness with which the satisfactory results were obtained in this research corresponds approximately to 15% of the individual thickness of the welded sheets–0.62 mm.

Finally, mention should be made of the characteristic appearance of these defects, in particular, the lack of vertical continuity and expulsion cavities. The first often produces a complete lack of fusion of the molten material through the inner surfaces of the sheets, the typical appearance being shown in Fig. 14a. Unlike those caused by coating evaporation, the cavities conserve some weld material at the interface area, as may be observed by comparison of Figs 14c and 10b.

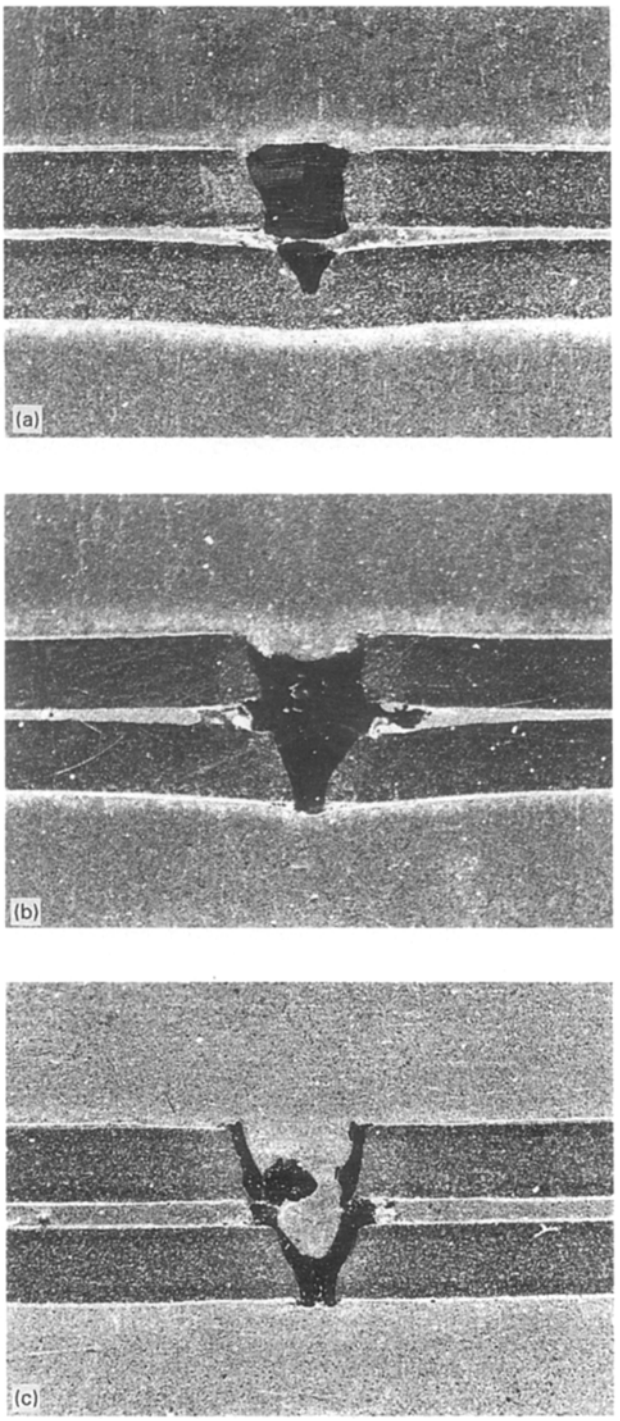

Figure 14 Welding laps made with 0.15 mm interface gap. Beam power of 1.5 kW and different welding speeds, V_s (m min^{-1}): (a) 3, (b) 2.5, (c) 2.

3.2.2. Butt welds

No clear evidence of the influence of the Al55–Zn coating was observed in either of the two thicknesses (0.62 and 1.16 mm) used for the butt welds. In general terms, the material behaves similarly to steel sheets without coating. A high degree of sensitivity of the procedure was observed, for example, in relation to the surface mismatching of the sheets, laser beam/joint alignment and excessively high or low laser beam power. Figs 15 and 16 are selected sections of certain welds in the 0.62 mm thickness, and show the effect of the aforementioned factors. Fig. 15a and b show, respectively, the effect of the first two factors independently one from the other, Fig. 15c showing their combined effect. In Fig. 15a the surface mismatch was approximately 10% of the thickness (0.06 mm) while in Fig. 15b misalignment of the beam was of the order of 0.015 mm. In both cases an important degree of undercutting may be observed. In Fig. 15c, with similar values for the two factors acting jointly, undercutting occurred on both sides of the joint.

Incorrect adjustment of the welding parameters also gave rise to defects in the welds, as may be seen in the sections shown in Fig. 16. As was observed in the study of the weld procedures, the power and speed suitable for the 0.62 mm thickness were 0.8 kW and

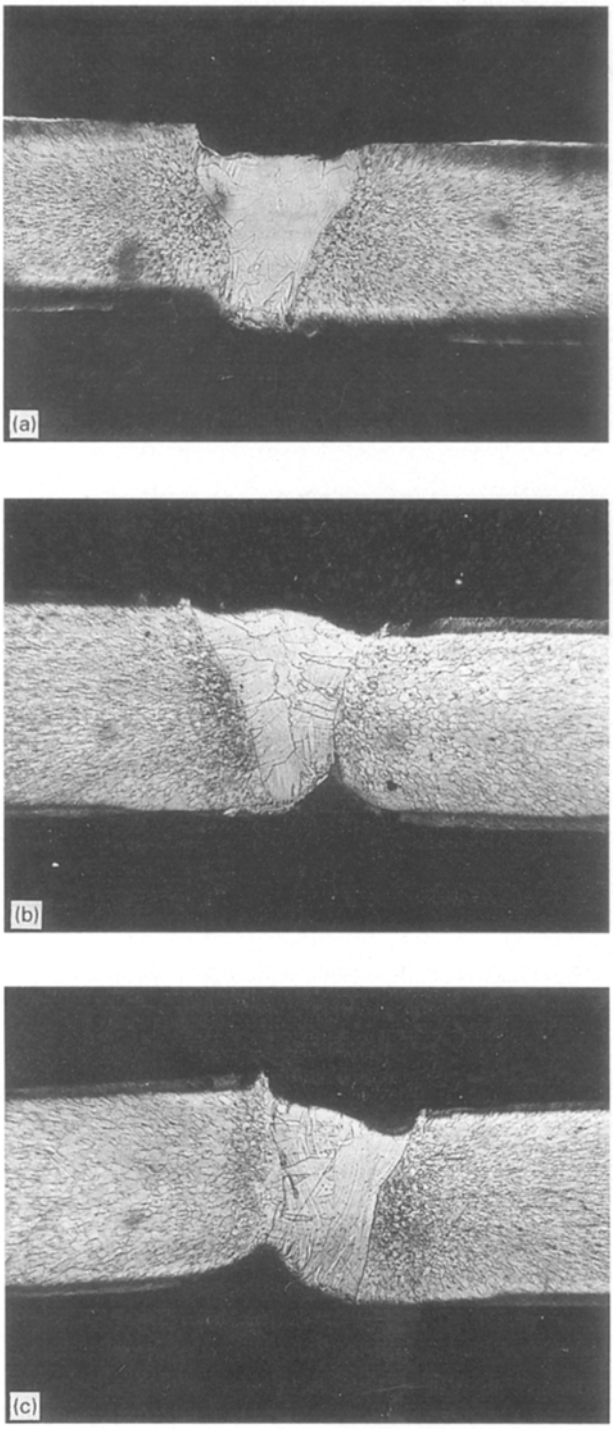

Figure 15 Butt welds in 0.62 mm thick sheets (a) Surface mismatching, 0.06 mm; (b) beam/joint misalignment, 0.15 mm; (c) conjunction of (a) and (b).

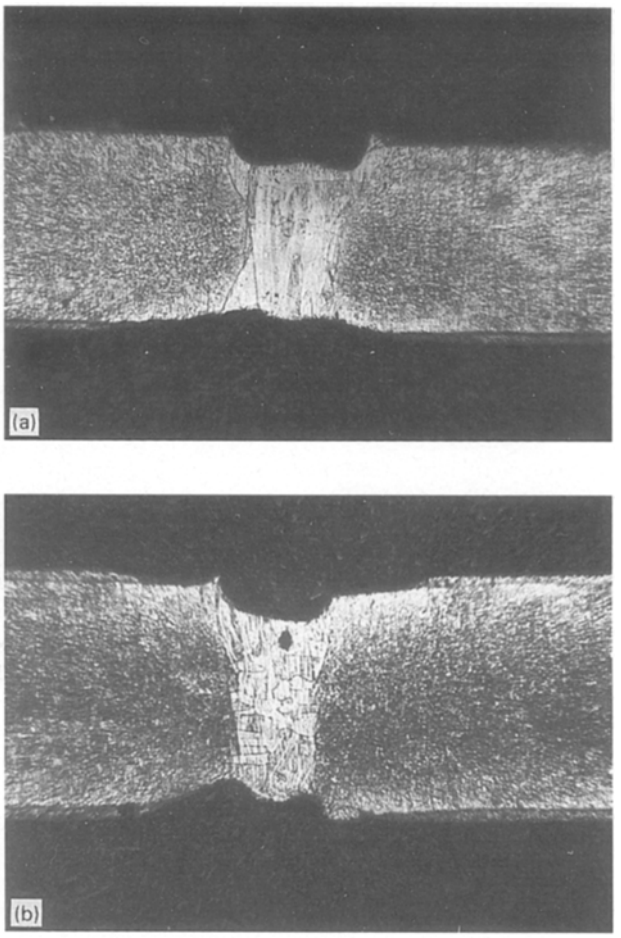

Figure 16 Effect of the beam power and welding speed. (a) Low power and speed, 0.7 kW, 3.4 m min^{-1}; (b) power and speed excessive, 1.1 kW, 4.2 m min^{-1}.

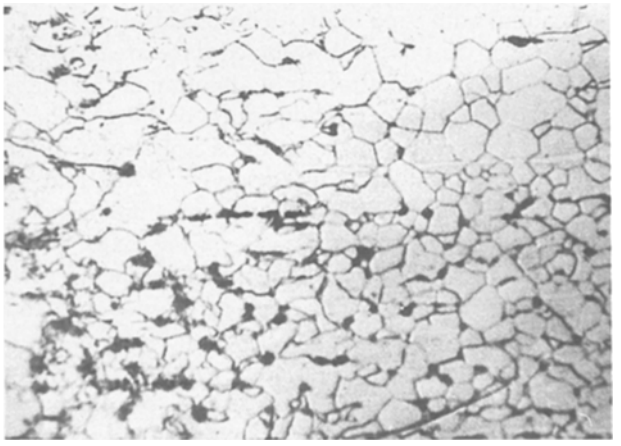

Figure 17 Cross-section of the coated material. Image resolution $\times 200$. Photographic scale 150:1.

3.5 m min^{-1}. In the weld shown in Fig. 16a, attempts were made to compensate the lower power of the beam by reducing the welding speed, this causing greater material loss at the weld surface and the underfill defect illustrated. In Fig. 16b, with higher power and speed than adequate, the undercutting which may be observed at the weld root occurred.

3.3. Microstructural analysis

Metallographic analysis of the coated material reveals a practically ferritic structure of the substrate, protected by a layer of Al55–Zn alloy of variable thickness, ranging from 30–50 μm. Fig. 17 shows a transverse section of the material to practically half the thickness; the wide variation of the grain size from the centre of the substrate to the coating (25–80 μm) may be observed.

A more detailed study of the coating, using a scanning electron microscope, reveals its structure in relation to its three components, aluminium, zinc and silicon. This is illustrated in Fig. 18, which shows a transverse section, (a), of the coating and the maps

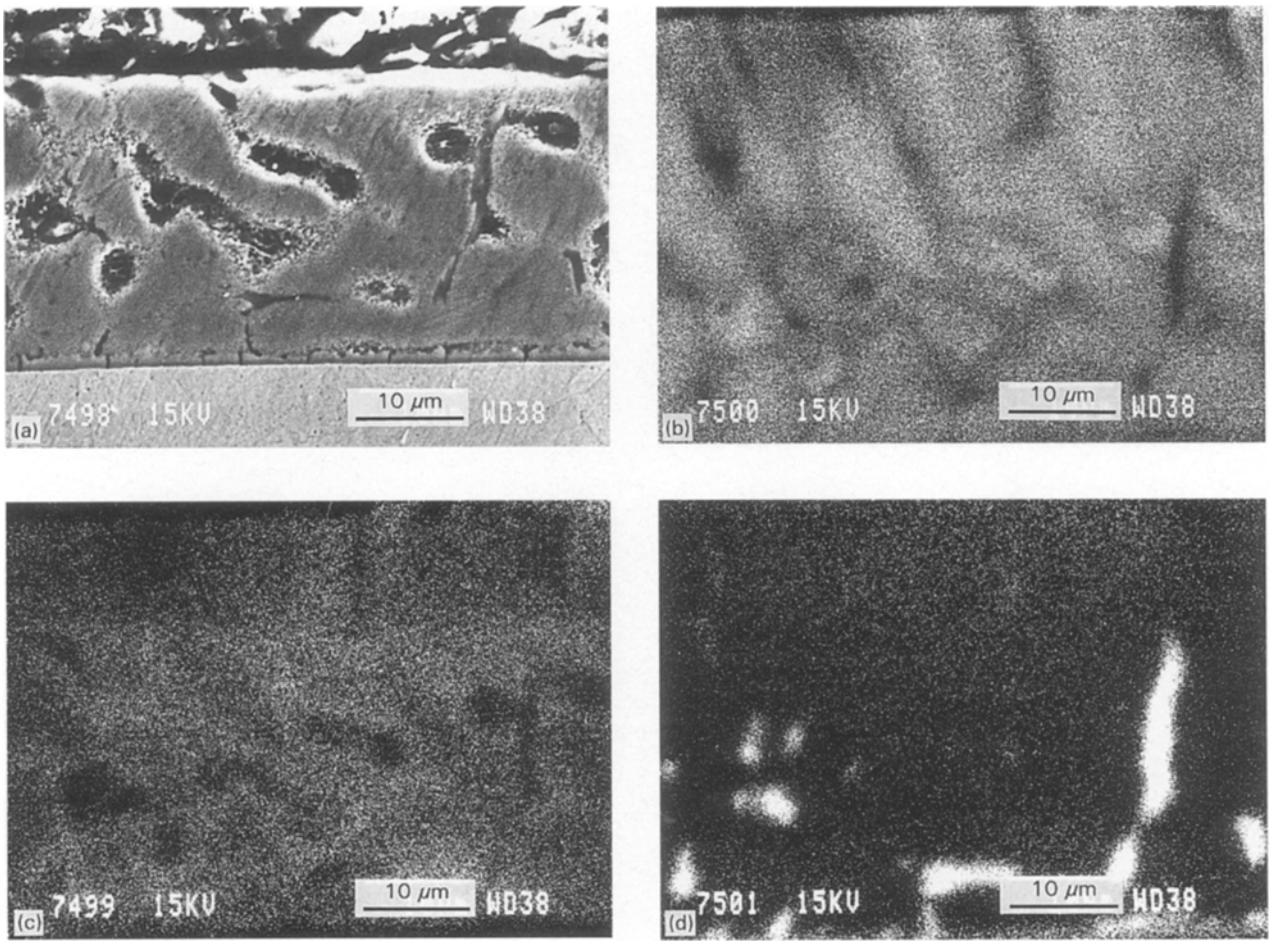

Figure 18 (a) Cross-section of the Al55–Zn coating (× 200). (b–d) Dispersive energy maps of (b) aluminium, (c) zinc and (d) silicon.

corresponding to dispersive energy analysis of the elements (b) aluminium, (c) zinc and (d) silicon. The aluminium–zinc matrix, composed of αAl + Zn phases may be observed; rounded dark areas appear with a higher concentration of aluminium, these corresponding to primary solidification of the αAl phase. Around these areas may be noted a granular phase with a slightly higher concentration of zinc and an acicular phase rich in silicon, clearly identifiable by the higher brightness of this element on the map.

The welded joints are characterized by the narrowness of the fusion and heat-affected zones (FZ and HAZ), these being of the order 0.6 and 0.8 mm in all cases. The X-ray spectrum taken towards the centre of the FZ of a butt weld on the 0.62 mm thickness (Fig. 19), reveals a composition fundamentally of iron, with a minimum participation of the elements aluminium and zinc. FZ also show symmetrical solidification to the central axis of the weld, with large ferritic grain sizes of up to 300 μm, as may be seen in the section shown in Fig. 20. This same type of structure may be seen in the 1.16 mm thickness and in the lap welds, with grains covering practically half the width of the FZ. Greater resolution shows certain perlitic colonies inside the ferritic matrix of the molten areas, as may be observed in the sections shown in Fig. 21a and b, with a tendency towards increasing numbers towards the centre of the welds. Fig. 22a shows the HAZ, the width of which may be estimated to be some 0.7 mm from the fusion line. Two clearly differentiated

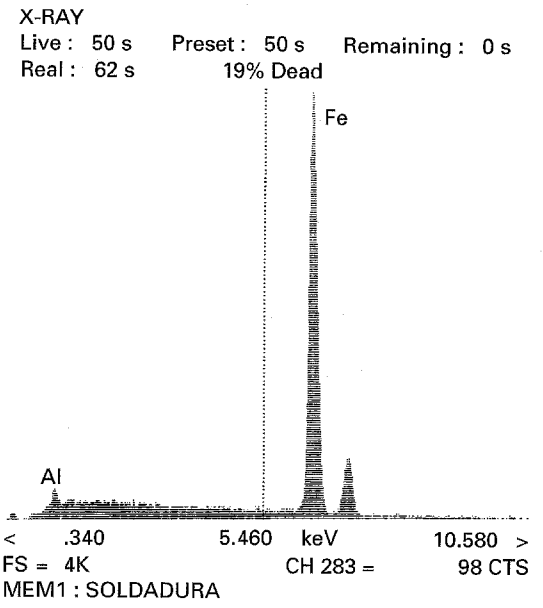

Figure 19 X-ray spectrum of the ZF of a butt weld.

areas may be distinguished inside this zone, one close to the fusion line with a bainitic microstructure, and a second close to the unaffected base metal, with a ferritic–perlitic microstructure, Fig. 22b and c.

The transverse hardnesses profile through the different joint areas reveals the moderate values achieved. The highest are located in the FZ, which is

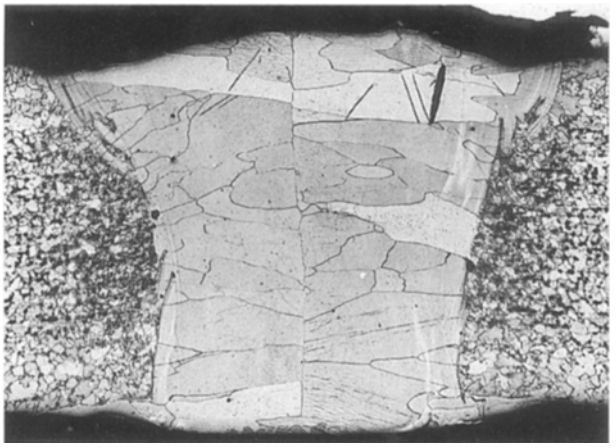

Figure 20 Butt weld macrosection (× 100).

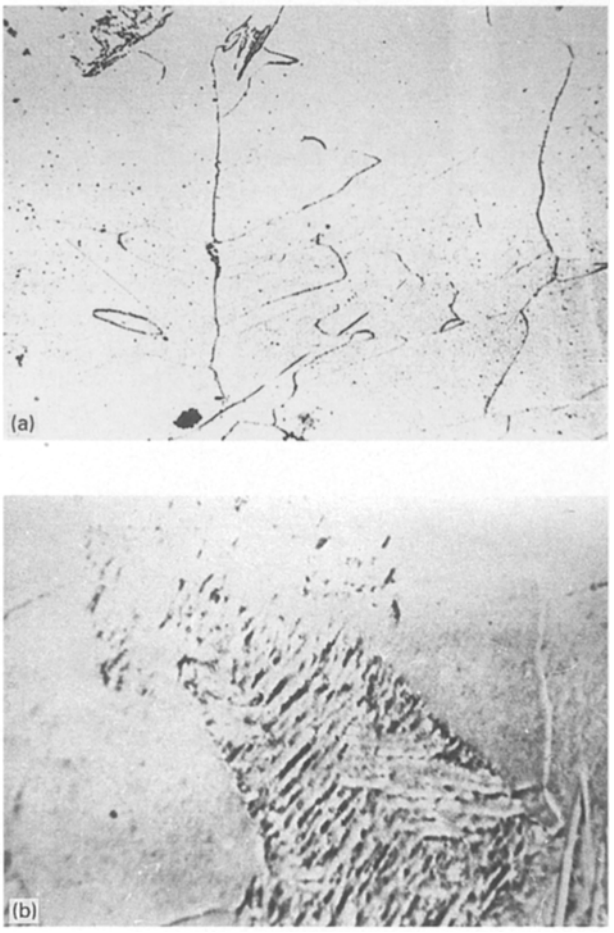

Figure 21 (a) Microstructure of the FZ. Image resolution (× 200). Photographic scale 150:1. (b) Enlargement of a perlite colony. Image resolution (× 500). Photographic scale 373:1.

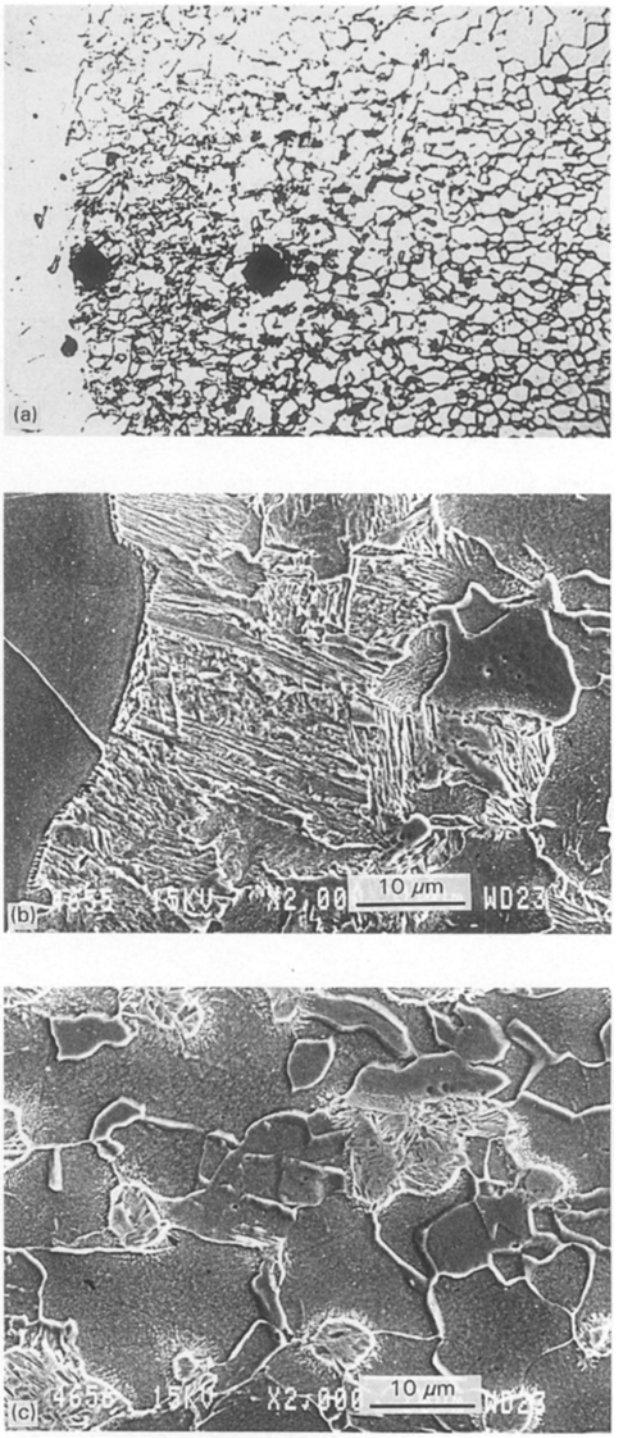

Figure 22 (a) HAZ microstructures. Image resolution (× 100). Photographic scale 75:1. (b) Bainitics close to the fusion line. (c) Ferritic–perlitic structures near the unaffected base metal.

normal in laser welding of this type of steel. This is reflected in the graph shown in Fig. 23, where it may be observed that values of 265 HV are reached in the FZ and values ranging from 200–240 HV in the HAZ, as against a value of 150 HV in the base metal.

The effect of the weld on the coating results in the elimination of the latter in the welded zone. A longitudinal band on either side of the weld of a width similar to that of the molten zone may be estimated to be destroyed by welding. Alongside these bands, the remaining coating shows gradual loss of thickness and metallurgical transformation of its original structure, as may be observed in the photograph shown in Fig. 24. Dispersive energy analysis of one of these transition zones is shown in Fig. 25. It may be observed that the darker areas continue to be rich in aluminium and slightly poorer in zinc in relation to the rest of the matrix. The most important effect is on the silicon, which is dissolved in the dark phases and disappears in its original acicular form.

Obviously, elimination of the coating occurs on both face and root in the case of butt welds or lap welds with total penetration. In partial penetration lap

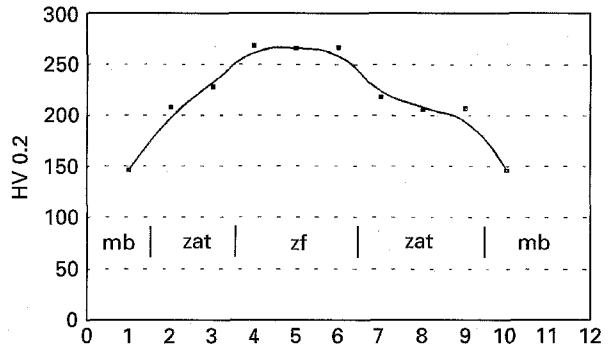

Figure 23 Hardness distribution across a welded joint.

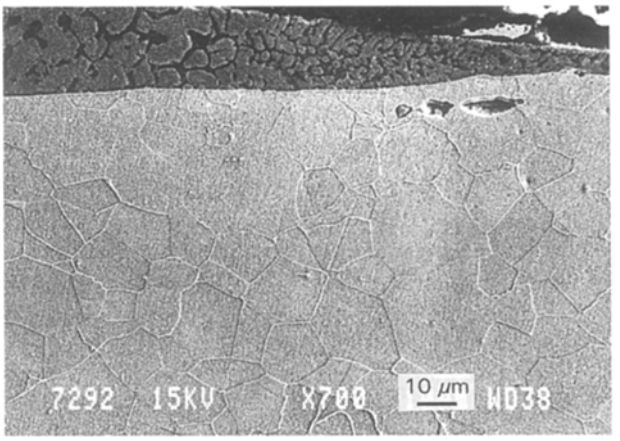

Figure 24 Gradual thickness loss and structural transformation of the coating.

welds, this loss occurs only on the upper surface, the coating being more or less affected on the lower surface depending on the proximity of the temperature reached to the transformation temperature.

4. Conclusions

1. The most important difficulties encountered in laser welding of sheets coated with the alloy Al55–Zn occurred in the case of lap joints. It was observed that as in other types of zinc-based coatings, the origin of the problems was vaporization of the coating zinc in the inner surfaces of the joints, the pressure of which lifted or expelled the molten metal, causing blistering or opened cavities seriously affecting the appearance and quality of the welds.

2. These difficulties are satisfactorily solved by inserting spacers between the sheets, such that an exit path is created for the vapours. It is important that a minimum interface gap compatible with vapour exit be maintained, because serious defects may occur with larger clearances. In the case of the 0.62 mm thickness used here, for example, acceptable welds were obtained with interface gaps of 0.1 mm, while gaps of

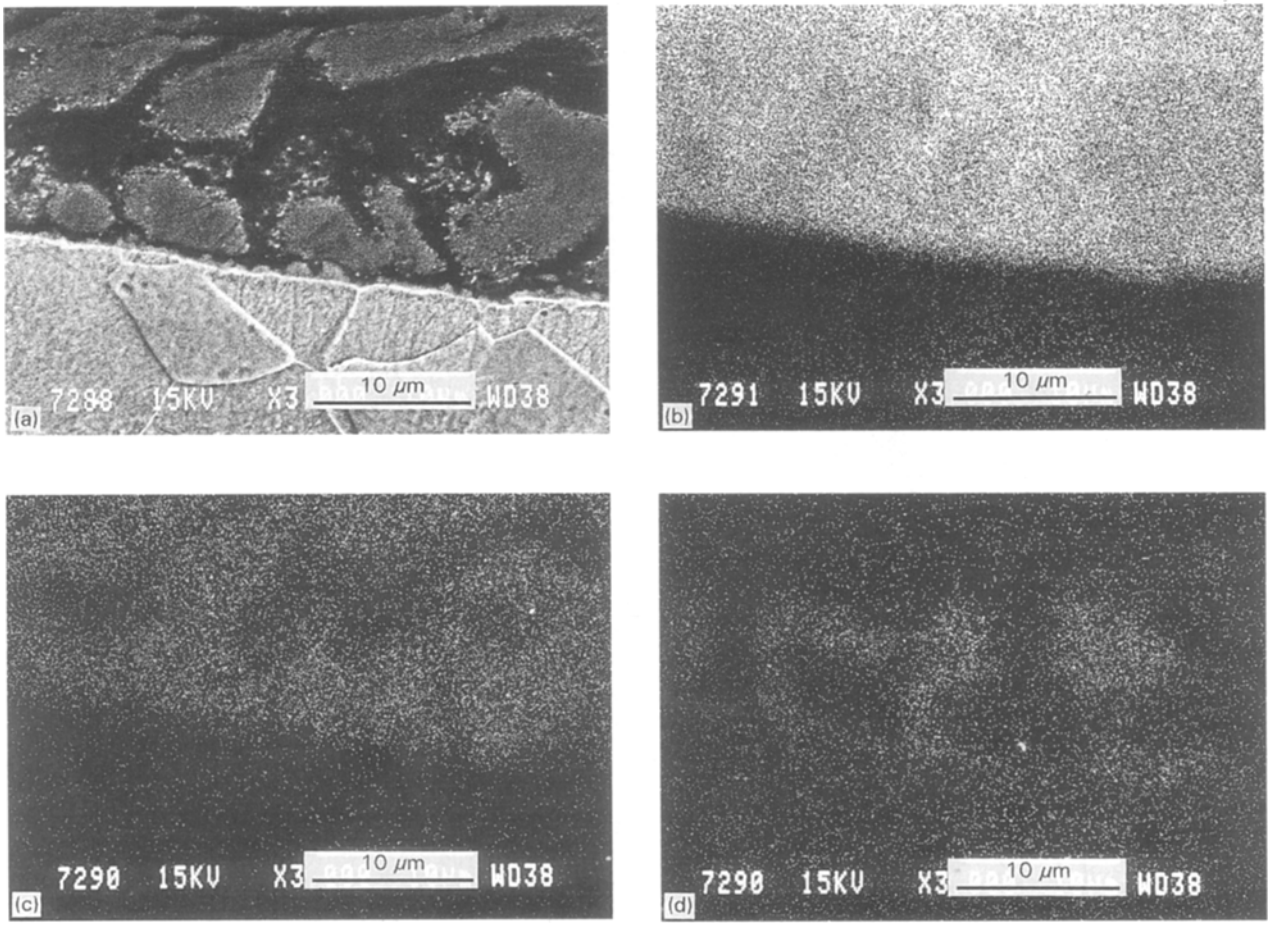

Figure 25 (a) TEM cross-section of the coating transition zone (× 3000) (b–d). Dispersive energy maps of (b) aluminium, (c) zinc, and (d) silicon.

0.15 mm caused important collapsing of the molten material and a lack of penetration.

3. No specific influence of the Al55–Zn coating was detected as regards the quality of the butt welds. The high sensitivity of the welding procedure to surface mismatching of the sheets or to laser beam/joint misalignment is a common characteristic with other types of coatings or with bare sheets.

4. Taking the previous considerations into account, the weldability of the material may be considered as being acceptable, this being confirmed in the metallographic analyses by the good continuity of the molten material, which is free from cracks, pores and inclusions. The mechanical properties of the welds are compatible with those of the base material, and moderate hardnesses, of less than 270 HV, are obtained in both the FZ and HAZ. Worthy of special mention is the large grain size in the molten areas, of up to 300 μm, and the narrowness of the HAZs, 0.6–0.8 mm, these being normal characteristics of laser welding of bare ferritic sheets or sheets with other types of coatings.

5. Nevertheless, the coating is eliminated on both sides of the weld, forming two longitudinal bands of a width approximately equal to the weld itself. At the edges of these bands, the coating undergoes a gradual loss of thickness and presents a recrystallized area having a different structure from the original. As the electron microscope analyses and energy dispersion maps revealed, the most heavily altered material is the silicon, which changes from its initial acicular structure to solid solution in the most aluminium–rich phase.

6. In the case of butt welds or total penetration lap welds, this elimination of the coating occurs on both faces of the bond, while in partial penetration lap welds it occurs only on the upper surface. There may, however, be damage to the lower surface, as well as alterations to the properties of the coating, depending on the temperature reached during welding.

Acknowledgements

The authors thank the Community of Madrid, which sponsored the project in relation to the present research, and the Technology Centre of Madrid (CETEMA), at whose installations the laser welds studied were carried out.

References

1. J. J. FRIEL and H. E. TOWNSEND, *Sheet Metal Ind.* **60** (1983) 506.
2. H. E. TOWNSEND, *Mater. Perform. Mag.* **26** (1987) 37.
3. N. T. WILLIAMS, *Weld. Metal Fabric.* **45** (1977) 275.
4. B. SCHMITZ and J. DEFOURNY, in "Proceedings of the 3rd International Conference on Trends in Welding Research", Gatlinburg, TN USA, June 1992, edited by S. A. David and J. M. Vitek (ASM International, Materials Park, OH, 1993) p. 427.
5. J. DURÁN, J. M. AMO and M. DEL TORO, Cenim-Ensidesa Research Project (1988).
6. R. S. BHATNAGAR, M. J. BINGAMAN and M. D. McSHANE, *Microstruct. Sci.* **20** (1993) 65.
7. T. NATALE and B. IRVING, *Weld. J.* **71** (1992) 47.
8. J. F. FLAVENOT, J. P. DEVILLE, A. DIBOINE, M. CANTELLO and S. L. GOBBI, *Weld. World* **31** (1993) 358.
9. 7210KB 431 Project, Ceca Research Program (1993).
10. CH. DAWES, "Laser Welding: a practical guide" (Abington, Cambridge, 1992).

Received 25 April
and accepted 23 November 1995